Development 133, 3451-3460 (2006) doi:10.1242/dev.02506

Primordial germ cell deficiency in the connexin 43 knockout mouse arises from apoptosis associated with abnormal p53 activation

Richard J. B. Francis and Cecilia W. Lo*

Connexin 43 knockout (Cx43α1KO) mice exhibit germ cell deficiency, but the underlying cause for the germ cell defect was unknown. Using an *Oct4-GFP* reporter transgene, we tracked the distribution and migration of primordial germ cells (PGCs) in the Cx43α1KO mouse embryo. Analysis with dye injections showed PGCs are gap-junction-communication competent, with dye coupling being markedly reduced in Cx43α1-deficient PGCs. Time-lapse videomicroscopy and motion analysis showed that the directionality and speed of cell motility were reduced in the Cx43α1KO PGCs. This was observed both in E8.5 and E11.5 embryos. By contrast, PGC abundance did not differ between wild-type and heterozygous/homozygous Cx43α1KO embryos until E11.5, when a marked reduction in PGC abundance was detected in the homozygous Cx43α1KO embryos. This was accompanied by increased PGC apoptosis and increased expression of activated p53. Injection of α-pifithrin, a p53 antagonist, inhibited PGC apoptosis and prevented the loss of PGC. Analysis using a cell adhesion assay indicated a reduction in β1-integrin function in the Cx43α1KO PGCs. Together with the abnormal activation of p53, these findings suggest the possibility of anoikis-mediated apoptosis. Overall, these findings show Cx43α1 is essential for PGC survival, with abnormal p53 activation playing a crucial role in the apoptotic loss of PGCs in the Cx43α1KO mouse embryos.

KEY WORDS: PGC, Cx43, Migration, p53, β1 integrin, Apoptosis, Mouse

INTRODUCTION

The connexin multigene family encode proteins that oligomerize to form gap junction membrane channels that span the extracellular space. They allow the direct transfer of ions, metabolites and other small second messengers between neighboring cells (Bruzzone et al., 1996; White and Paul, 1999). The connexin gene *Gja1* encodes a 43 kd protein known as connexin 43 or Cx43 (Goodenough et al., 1996; Sohl and Willecke, 2004), also known as α_1 connexin (Kumar and Gilula, 1996), and is referred to here as Cx43α1. Studies of knockout mouse models have revealed an essential role for a number of the connexins in development and disease (White and Paul, 1999). Cx43α1 was shown to be essential in heart development, as the Cx43α1 knockout mice *Gja1*^{tm1Kdr} (Cx43α1KO) die at birth due to conotruncal heart malformations and pulmonary outflow obstruction (Reaume et al., 1995). Cx43α1KO mice also displayed gonadal defects, with newborn pups exhibiting hypoplastic ovaries and testes deficient in primordial germ cells (PGCs) (Juneja et al., 1999; Roscoe et al., 2001).

In mouse embryos, cytochemical detection of alkaline-phosphatase activity indicated that PGCs first appear at embryonic day (E) 7.0, in the extra-embryonic mesoderm at the base of the allantois (Bendel-Stenzel et al., 1998). However, PGCs may be linage specified earlier, as PGCs emerge when epiblasts from E5.5 embryos are co-cultured with extra-embryonic ectoderm (Yoshimizu et al., 2001). From the allantois, PGCs migrate into the hindgut endoderm (E8.0), and travel along the dorsal mesentery (E9.5), finally arriving at and populating the genital ridges (E10.5-E11.5) (Bendel-Stenzel et al., 1998; McLaren, 2003). From a founding population of about ten cells at E7.0 (Ginsburg et al., 1990), PGCs rapidly expand to approximately 25,000 cells at E13.5, when gonadal differentiation begins in conjunction with sex determination (Tam and Snow, 1981). Recent studies have provided extensive evidence of an essential role for Cx43α1 in gonadogenesis. Cx43α1 is seen at all stages of ovary development (Perez-Armendariz et al., 2003) and is required for the growth and expansion of granulosa cells. Ovaries in the Cx43α1KO mice are PGC deficient (Juneja et al., 1999). In the absence of Cx43α1, granulosa cells are not functionally coupled and stop growing at an early pre-antral stage (Gittens et al., 2003). Lack of Cx43α1 restricted to the granulosa cells is sufficient to prevent the normal development of both oocyte and follicle, but chimera studies showed that Cx43α1 expression in oocytes is not required for oocytes to reach maturity (Gittens and Kidder, 2005). These findings indicate an essential role for Cx43α1 in folliculogenesis. Cx43α1 is also found at all stages of testicular development, and provides gap junctions that link germ cells with Sertoli cells (Perez-Armendariz et al., 2001). Testes isolated from Cx43α1-deficient fetuses display a 'Sertoli cell only' phenotype characterized by an almost complete lack of germ cells (Roscoe et al., 2001).

Cx43α1KO embryos are known to be PGC deficient from E11.5, the time when genital ridges are first formed (Juneja et al., 1999). This would suggest an early requirement for Cx43α1 in germ cell development. Actively migrating PGCs are known to form extensive cell-cell contacts, such that more than 90% of the migrating PGCs are linked via cell processes (Gomperts et al., 1994). This suggests the possibility that cell-cell interactions mediated by Cx43α1 may play a role in regulating the migration and targeting of PGCs to the genital ridge. We previously showed Cx43α1 modulates the migratory behavior of two extracardiac cell populations, the cardiac neural crest (Huang et al., 1998; Sullivan et al., 1998; Xu et al., 2001) and pro-epicardial cells (Li et al., 2002). Thus it seemed plausible that the PGC deficiency of the Cx43α1KO mouse may involve a germ cell migration defect due to the loss of Cx43α1 gap

Laboratory of Developmental Biology, National Heart Lung and Blood Institute, National Institutes of Health, Building 50/Room 4537, 9000 Rockville Pike, Bethesda, MD 20892, USA.

*Author for correspondence (e-mail: loc@nhlbi.nih.gov)

Accepted 21 June 2006

junction contacts. To investigate this, we utilized an *Oct4* (*Pou5f1* – Mouse Genome Informatics) promoter-driven GFP transgene as a marker for tracking PGCs in the mouse embryo (Yoshimizu et al., 1999). *Oct4* encodes a transcription factor belonging to the POU family of proteins. Its promoter has been used to drive PGC-specific gene expression (Pesce and Scholer, 2001). An *Oct4-GFP* transgene has been shown to be an ideal marker for PGCs spanning E8.5 to E11.5 (Yoshimizu et al., 1999). The transgene is initially expressed ubiquitously from the morula stage, but at E8.0 its expression becomes restricted to PGCs at the base of the allantois, remaining PGC restricted until E14.5, when expression in female gonads is significantly downregulated (Yoshimizu et al., 1999). This pattern of transgene expression closely matches the expression pattern of endogenous *Oct4* transcripts observed by whole-mount in situ hybridization analysis (Kawase et al., 2004). Using the *Oct4-GFP* transgene, we tracked PGC migration in the E8.5 to E11.5 mouse embryos. With microelectrode impalements into GFP-expressing PGCs, we showed that migrating PGCs make functional gap junction contacts with surrounding cells. We found no difference in the distribution or abundance of PGCs in wild type versus homozygous/heterozygous Cx43α1KO mouse embryos from E8.5 to E10.5. However, at E11.5, there was a marked loss of PGC in the homozygous Cx43α1KO mouse embryos. Although Cx43α1-deficient PGCs showed decreased cell motility, PGCs from the heterozygous and homozygous Cx43α1KO mouse embryos showed the same change in cell motile behavior. By contrast, studies using TUNEL labeling indicated an abnormal elevation of apoptosis only at E11.5, the time when PGC deficiency is first detected in the Cx43α1KO embryos. This was associated with an abnormal elevation of activated p53, and injections with a p53 antagonist, α-pifitrhin, into pregnant mice prevented the loss of PGCs in the Cx43α1KO embryo. p53 is known to mediate apoptosis associated with integrin-mediated anoikis (Wang et al., 2002; Zhang et al., 2004), and using a cell adhesion assay, we further showed β1-integrin-mediated adhesion was reduced in Cx43α1-deficient PGCs. Together these findings indicate that Cx43α1 is required for germ cell survival, with Cx43α1-deficient PGCs undergoing apoptosis in a p53-dependent manner.

MATERIALS AND METHODS

Mouse breeding and genotyping

All experiments were conducted in accordance with an approved animal protocol of the National Heart Lung Blood Institute (Protocol Number H-0086). All experiments were carried out using embryos obtained from the mating of heterozygous Cx43α1KO mice that were homozygous for the *Oct4-GFP* transgene (Yoshimizu et al., 1999). Embryonic day 0.5 (E0.5) refers to the day the vaginal plug was found. Cx43α1 genotyping was conducted as previously described (Xu et al., 2001).

Analysis of PGC distribution and abundance in whole-mount specimens

Embryos were collected at E8.5 to E11.5 and fixed overnight at 4°C in 10% formalin. For E9.5 to E11.5 embryos, the left body wall was dissected free before fixation to facilitate PGC visualization. The following day embryos were washed 3× in PBS, and embedded in 2% agarose in 35 mm Petri dishes. E8.5 embryos were positioned primitive streak side down to allow easy visualization of PGCs at the base of the allantois and in the prospective hindgut. Embryos at E9.5 to E11.5 were placed on their right side to facilitate visualization of PGCs in the hindgut, hindgut/developing genital ridge, and genital ridge, respectively. Embryos were viewed under a Leica DMLFSA microscope with a water immersion lens and a 100-watt mercury lamp using GFP filters (425/60 nm excitation and 480 nm emission). For quantitation of PGC abundance, whole-mount fluorescence images were captured for embryos of the same developmental stage using a uniform imaging protocol. This involved capturing *z*-stacks consisting of an identical number of optical slices (see below) under the same magnification, and using identical camera settings and exposure time. The highest magnification was used at each developmental stage to allow visualization of all of the PGC-containing tissue in the embryo – i.e. the allantois for E8.5, hindgut for E9.5-E10.5 and genital ridge for E11.5. Under these conditions, the relative abundance of PGC in embryos at the same developmental stage can be directly compared via the mean intensity of GFP fluorescence per unit area (i.e. average brightness/pixel). For these quantitative assessments, 500 μm image stacks were obtained via 75 optical slices using an ORCA-ER digital camera (Hamamatsu). The image stacks were deconvolved using Openlab volume deconvolution (Openlab 3.1.7, Improvision), then merged to generate a single 2D image, from which the mean fluorescence intensity was determined using Openlab. To assess PGC distribution along the hindgut, E9.5 stage embryos were collected and fixed overnight in 10% formalin at 4°C. The following day brightfield and GFP fluorescent images were taken using a Leica MZFLIII stereomicroscope. Somites were used as morphological landmarks to assess PGC abundance along the hindgut. Maximal PGC migration distance was also determined by measuring the distance from the base of the allantois to the PGC migration front situated rostrally along the anterior hindgut.

Time-lapse videomicroscopy of live tissue explants

For time-lapse imaging of E8.5 embryos, the caudal end of the embryo spanning the base of the allantois was embedded in a thin layer of agarose ventral side up in a 35 mm Petri dish using low melt agarose. For E11.5 embryos, tissue explants containing the genital ridge were obtained by dissecting free a short abdominal section of the embryo spanning the developing fore and hindlimb buds. After removing one side of the body wall, the tissue was embedded in low melt agarose with the exposed body wall facing up, allowing easy viewing of the PGCs in the genital ridge. To embed the dissected tissue in low melt agarose, the Petri dish was chilled on ice for 45-60 seconds to set the agarose, after which 4-5 ml of pre-warmed (37°C) L-15 medium was added. The explants were imaged as above using darkfield epifluorescence illumination under a Leica DMLFS microscope. A small amount of mineral oil (Sigma) was used to cover the medium to prevent evaporation. Temperature was maintained at 37.0±0.5°C using a Peltier heated stage (Omega, CT). To further ensure temperature stability, an air curtain was maintained around the microscope using two heating fans (Nevtek, VA). Time-lapse images were captured under darkfield illumination. *Z*-image stacks were obtained comprising 11-13 μm slices spanning 165-220 μm thickness captured every 6 minutes over 6-8 hours. To minimize phototoxicity, epifluorescent illumination was reduced by using a neutral density filter and a UV cutoff filter to block transmission below 400 nm. Exposure time was minimized, with each embryo having a cumulative exposure of ~140 seconds over the course of 8 hours. Image stacks were processed by volume deconvolution and subsequently merged into a single 2D image for fluorescence quantitation. These serial 2D images were used to calculate the speed and directionality of cell motility, assessed using the measurements module of Volocity (Volocity 3.5, Improvision Ltd). Directionality is derived from the net migration distance achieved divided by the total real distance traveled. It measures the degree to which the migratory path strayed from a straight line, with a maximal directionality of 1 corresponding to a cell moving in a straight line, while a cell meandering extensively from a straight path would have a directionality much less than 1.

Apoptosis and cell proliferation analyses

PGC apoptosis was first examined using a sulforhodamine poly-caspase-binding kit (ATCC, Manassas, VA). This entailed culturing embryo explants with a cell permeable and noncytotoxic sulforhodamine derivative of valylalanylaspartic acid fluoromethyl ketone that binds and fluorescently labels caspases 1, 3, 4, 5, 6, 7, 8 and 9. Further analysis was carried out using TUNEL labeling. For these studies, E11.5 genital ridges were fixed in 2% paraformaldehyde (20 minutes), followed by three washes in PBS and permeabilization overnight with PBT (PBS with 10% FBS and 0.2% Titron X-100) (12+ hours at 4°C). The following day, the genital ridges were processed using an APO-BrdU TUNEL Assay Kit from Invitrogen (Carlsbad, CA) using the manufacturer's specifications.

For cell proliferation analysis, pregnant mice at E11.5 gestation were injected intraperitoneally with 3 mg/ml BrdU (1 ml/100 g body weight; Zymed Laboratories, San Francisco, CA). After 45 minutes, the embryos were harvested and the genital ridges retrieved, fixed in 2% paraformaldehyde (20 minutes), washed in PBS (×3), followed by PBS containing 10% FBS, then permeabilized with PBT overnight. The following day the genital ridges were incubated for 30 minutes with the denaturation solution supplied in the Zymed BrdU staining kit (Zymed Laboratories Inc., San Francisco, CA). BrdU detection for both TUNEL and cell proliferation analyses was carried out using an anti-bromodeoxyuridine monoclonal antibody conjugated with Alexa Fluor 546 (Invitrogen, Carlsbad, CA), and visualized using a Cy3 fluorescence filter (535/50 nm excitation and 610/75 nm emission).

PGC dye-coupling analysis

To quantitate dye coupling in PGCs, hindgut explants from E9.5 embryos were isolated and cultured on coverslips overnight in DMEM containing 10% FBS, 100 U/ml penicillin/streptomycin, and supplemented with growth factors (2 ng/ml TNF-α and 50 ng/ml soluble SCF from RD Systems Minneapolis, MN; and 10 ng/ml LIF from Chemicon International, Temecula, CA). For dye injection, coverslips were secured to the bottom of 35 mm culture dishes using a small amount of silicon grease, and L-15 medium containing 10% FBS added to the dish. The dish was then placed on a heated stage of a Leica DMLFSA microscope for microelectrode impalements. Micropipettes were pulled from borosilicate capillary glass (with filament O.D. 1 mm, I.D. 0.58 mm) using a model P-97 Flaming/Brown micropipette puller (Sutter Instruments, Novato, CA) and back-filled with sulforhodamine 101 dye (12.5 mg/ml, Invitrogen, Carlsbad, CA). *Oct4-GFP*-expressing PGCs were iontophoretically injected with sulforhodamine 101 dye for 2 minutes using 0.5 nA current pulses at 1 Hz. Dye spread was observed for a further 3 minutes following cessation of iontophoresis. Dye spread was quantified by measuring total dye spread area.

β1-integrin-function-blocking antibody treatment on PGC migration

Tissue from the base of the allantois was isolated from E8.5 embryos containing the *Oct4-GFP* transgene, and cultured overnight in 8-chamber glass slides (BD Biosciences, San Jose, CA) with DMEM containing 10% FBS and supplemented with growth factors as described above. The following day the culture medium was replaced with L-15 medium with the same growth factors and covered with a thin layer of paraffin oil to prevent evaporation. Rat monoclonal anti-mouse β1-integrin-function-blocking antibody (1:200 dilution; BD Biosciences, San Jose, CA) was added and the explant was then examined by time-lapse imaging. Image stacks comprised 15-20 optical slices (11-13 μm *z*-steps) were captured every 8 minutes over 6-8 hours. Image stacks were deconvolved, merged into a single 2D image, and the 2D images spanning the time-lapse interval were used to analyze the speed and directionality of PGC cell migration using Volocity (Volocity 3.5, Improvision, Ltd, UK).

Assessment of β1-integrin-mediated adhesion

β1-integrin-mediated adhesion was assessed using a Chemicon cell adhesion assay (Temecula, CA). Genital ridges were isolated from E11.5 embryos, incubated for 20 minutes in PBS containing 0.5 mg/ml collagenase/dispase (Sigma, St Louis, MO), then washed in PBS and transferred into 200 μl of DMEM with 10% FBS (per genital ridge). This was followed by gentle aspiration with a 1 ml pipette, and the disaggregated cells were then placed in wells pre-coated with a β1-integrin antibody (Chemicon Kit ECM522). After 2 hours' incubation (5% CO_2, 37°C), five random areas from each well were imaged using a 10× objective under darkfield illumination to quantitate the number of bound PGCs. The wells were then washed with 1 ml of PBS, after which another five random areas from each well were imaged. The number of PGCs remaining was counted, and the percent of bound PGCs after washing was calculated to compare the relative level of β1-integrin adhesion in wild-type, heterozygous, and homozygous Cx43α1 KO PGCs.

Treatment with α-pifithrin

Pregnant female mice at E10.5 gestation were injected intraperitoneally with either α-pifithrin (2.2 mg/kg, Calbiochem, La Jolla, CA) or vehicle (DMSO/0.9% NaCl) at midday and again at midnight before harvesting at E11.5. The genital ridges were retrieved and GFP fluorescence, TUNEL labeling and PGC proliferation were assayed as described above. To examine the expression of activated p53, E11.5 genital ridges were fixed in 4% paraformaldehyde for 20 minutes, then washed and incubated with antibody to phosphoSer^{15}-p53 (Cell Signaling Technology, Inc., Danvers, MA) at 4°C overnight, followed by incubation with a Cy3-conjugated secondary antibody. Epiflourescence imaging was carried out on a Leica DMRE microscope with a 40× objective.

Statistical analyses

Our results were expressed as mean ± standard error of the mean, with the statistical analyses carried out using the InStat software package (3.0b, GraphPad Software, Inc.). Differences between genotypes were compared using unpaired analysis of variance (ANOVA), while the means of all three genotypes were compared using the Bonferroni test. $P<0.05$ was considered statistically significant.

RESULTS

Gap junction communication in PGCs

Although PGCs are known to express Cx43α1, whether PGCs are gap-junction-communication competent is unknown. To examine the gap-junction-communication competency of PGCs, we carried

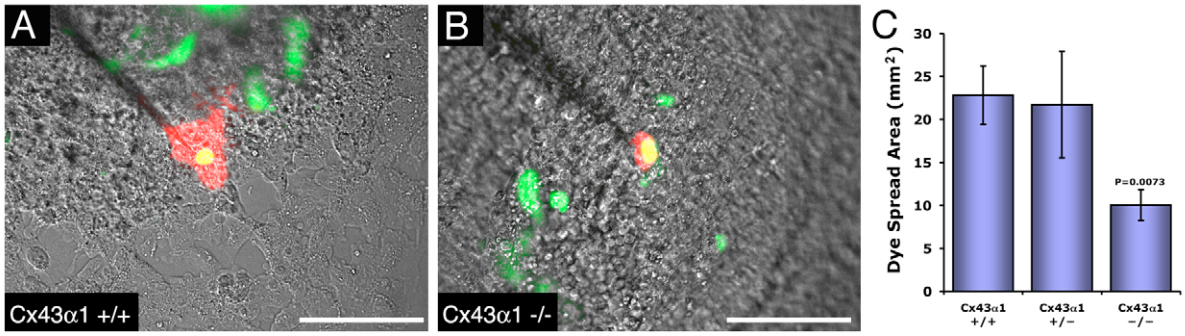

Fig. 1. Dye coupling of PGC cells with their neighbours. (**A**,**B**) Representative images obtained following intracellular microinjection of fluorescent dye sulforhodamine 101 into PGCs contained in hindgut explants from both Cx43α1 wild-type (+/+) and homozygous Cx43α1KO (–/–) embryos (E9.5). Both A and B comprise three images superimposed: a DIC image, green *Oct4-GFP* fluorescence image (PGC), and a red sulforhodamine 101 fluorescence image. (**C**) Dye spread was quantified by calculating total area of dye spread after 5 minutes (2 minutes' active microinjection plus 3 minutes' passive spread). PGCs in Cx43α1KO (–/–) explants displayed a significant reduction in their ability to pass dye into their neighbors. For this analysis, 8, 4 and 7 microelectrode impalements were carried out, respectively in four Cx43α1 +/+, four Cx43α1 +/– and five Cx43α1 –/– embryo explants.

out microelectrode impalements and iontophoretic injections of sulforhodamine 101 into *Oct4-GFP*-expressing PGCs in E9.5 hindgut tissue explants (Fig. 1). Sulforhodamine 10l is a gap junction permeable fluorescent dye of 607 daltons. It has excitation/emission wavelengths separable from GFP, and thus can be distinguished from the GFP fluorescence used to label the PGCs. In wild-type embryos, the injected dye spread readily from the impaled GFP-expressing PGC into surrounding non-GFP-expressing cells (Fig. 1A). Although dye transfer was never observed directly between PGCs, we note that PGCs were generally very sparsely distributed in the E9.5 hindgut explants. The extent of dye spread was quantitatively assessed by measuring the total area of dye spread (Fig. 1C). Similar analysis of PGCs in homozygous Cx43α1KO explants also showed dye spread, but the extent of spread was significantly reduced when compared with wild-type and heterozygous KO embryos. These observations show that migrating PGCs are well coupled to surrounding cells via gap junctions. They suggest that Cx43α1 plays a significant, but not exclusive, role in mediating gap junctional communication in migrating PGCs.

Distribution and abundance of PGCs

To determine if the distribution and abundance of PGCs may be perturbed by the loss of Cx43α1 function, Cx43α1KO mouse embryos from E8.5 to E11.5 were examined by epifluorescence imaging to visualize the migrating PGCs. At E8.5, the GFP-expressing PGCs can be seen in the caudal aspect of the embryo, at E9.5/E10.5 in the region spanning the hindgut, and at E11.5, the genital ridge (Fig. 2). This same pattern was observed in wild-type and heterozygous/homozygous Cx43α1KO mouse embryos. To determine whether there may be changes in PGC abundance with Cx43α1 deficiency, we quantitatively assessed the GFP fluorescence in wild-type, heterozygous and homozygous Cx43α1KO mouse embryos from E8.5 to E11.5. No difference was detected between wild-type, heterozygous, and homozygous KO embryos at E8.5, E9.5 or E10.5 (Table 1). However, at E11.5, GFP fluorescence in the homozygous Cx43α1KO mouse embryos was markedly reduced compared with wild-type and heterozygous KO embryos (Table 1). This difference was evident even by direct visual observation of the genital ridges (Fig. 2). The decrease in GFP fluorescence is not due to changes in intrinsic GFP fluorescence in the Cx43α1-deficient PGCs, as GFP fluorescence intensity in individual PGCs, whether wild type or Cx43α1 deficient, was indistinguishable (data not shown).

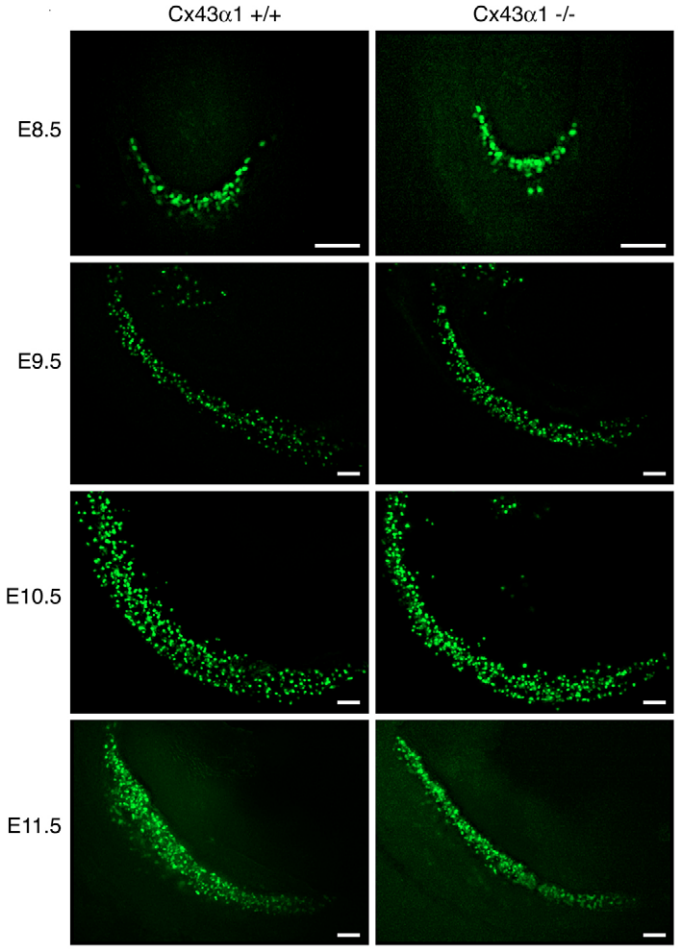

Fig. 2. PGC distribution in the Cx43α1 KO mouse embryo. The distribution of PGCs in Cx43α1 wild-type (+/+) and homozygous Cx43α1KO (–/–) mouse embryos from E8.5 to E11.5 was observed via GFP expression mediated by an *Oct4-GFP* transgene. No difference was seen in the overall distribution of GFP-expressing cells in the wild-type versus KO mouse embryos. However, at E11.5 there was a noticeable reduction in GFP fluorescence in the genital ridges of the KO mouse embryos. Scale bars: 100 μm.

Analyses of PGC migration and motile behavior

To examine if PGC motility may be altered by Cx43α1 deficiency, we used time-lapse videomicroscopy with darkfield epifluorescent illumination to visualize the migratory paths of GFP-expressing PGCs in E8.5 and E11.5 tissue explants. For E8.5 embryos, time-lapse movies were generated using explants from the caudal PGC-containing region of the embryo (see Movie S1 in the supplementary material), while for E11.5 embryos, time-lapse movies were obtained from the explanted genital ridge. Images were captured every 6 minutes over a 6-8 hour interval. Quicktime movies generated from the darkfield images were used to trace the migratory paths of individual PGCs (Fig. 3A,B). Using these migratory paths, we carried out quantitative motion analysis to obtain the speed and directionality of cell movement. Directionality measures the degree to which the migratory path of a cell strayed from a straight line, with a maximal directionality of 1 corresponding to a cell moving in a straight line (see Materials and methods). This analysis showed that in wild-type PGCs the speed of cell locomotion is markedly decreased from E8.5 to E11.5, going from approximately 18 μm/hour to 10 μm/hour, while the directionality of cell movement showed little change (Fig. 3C,D). This reduction in speed is consistent with the results of a previous study that recorded PGC migration in 2D tissue slices taken from embryos embedded in agarose (Molyneaux et al., 2001). The Cx43α1KO PGCs also showed reductions in the speed and directionality of cell movement at E8.5 and E11.5. However, at each embryonic stage, the heterozygous and homozygous KO PGCs exhibited lower speed and directionality of cell movement than those exhibited by the wild-type PGCs. Note that the speed and directionality of cell movement in the heterozygous and homozygous Cx43α1KO PGCs were indistinguishable (Fig. 3C,D).

To ascertain if these reductions in the speed and directionality of cell movement may affect the targeting of PGCs along their normal migratory path to the genital ridges, we used somites as morphological landmarks to assess the abundance of PGCs in the hindgut of E9.5 embryos (Fig. 4). Quantitative assessment of GFP

Table 1. Changes in PGC abundance in Cx43α1 KO mouse embryos

	Mean GFP fluorescence			
Genotype	E8.5	E9.5	E10.5	E11.5
Cx43α1 +/+	301±35 (*n*=6)	547±30 (*n*=7)	689±59 (*n*=5)	770±27 (*n*=4)
Cx43α1 +/–	272±27 (*n*=7)	532±21 (*n*=10)	703±45 (*n*=10)	704±50 (*n*=7)
Cx43α1 –/–	290±29 (*n*=3)	550±14 (*n*=5)	724±53 (*n*=3)	539±30* (*n*=5)

**P*=0.0008 versus stage-matched wild-type embryos.

fluorescence intensity along the hindgut of E9.5 embryos showed a similar distribution of PGCs in the wild-type and Cx43α1 heterozygous/homozygous KO mouse embryos (data not shown). We further assessed the maximal migration distance of PGCs along the hindgut of E9.5 Cx43α1KO mouse embryos. This entailed measuring the distance from the base of the allantois (Fig. 4B, arrowhead), the region from which PGCs arise, to the migration front at the anterior end of the hindgut (Fig. 4B arrow). We found no difference in the migration distance achieved by PGCs, whether wild type, heterozygous or homozygous Cx43α1KO, the maximal distances being 1.11±0.02 mm for wild-type, 1.11±0.06 mm for heterozygous and 1.16±0.05 mm for homozygous Cx43α1KO embryos.

Analysis of PGC proliferation and apoptosis

While examining the time-lapse movies, we observed PGCs undergoing mitotic cell division (see Movie S2 in the supplementary material). In addition, some PGCs were observed to fragment and disintegrate (see Movie S3 in the supplementary material). Shown in Fig. 5 are images from a time-lapse movie showing the progressive fragmentation of a PGC (Fig. 5A). Immunostaining using a poly-caspase marker showed that these cell fragments were caspase-positive, suggesting that they may represent apoptotic cells (Fig. 5B). To compare the rate of PGC proliferation or apoptotic cell death in wild-type versus Cx43α1KO embryos, we counted the number of mitotic and fragmenting cells observed in the time-lapse movies. An apoptotic index generated by normalizing the number of apoptotic cells by the number of mitotic cells showed more than twofold increase in the relative incidence of apoptosis in the homozygous KO PGCs (Fig. 5C).

To assess the incidence of apoptosis directly, we carried out TUNEL assays. Consistent with the findings from the time-lapse movies, these studies showed a significant increase in TUNEL labeling in PGCs of homozygous Cx43α1KO mouse embryos (Fig. 6D-F). We also quantitatively assessed PGC proliferation by examining BrdU incorporation in the E11.5 genital ridges. In

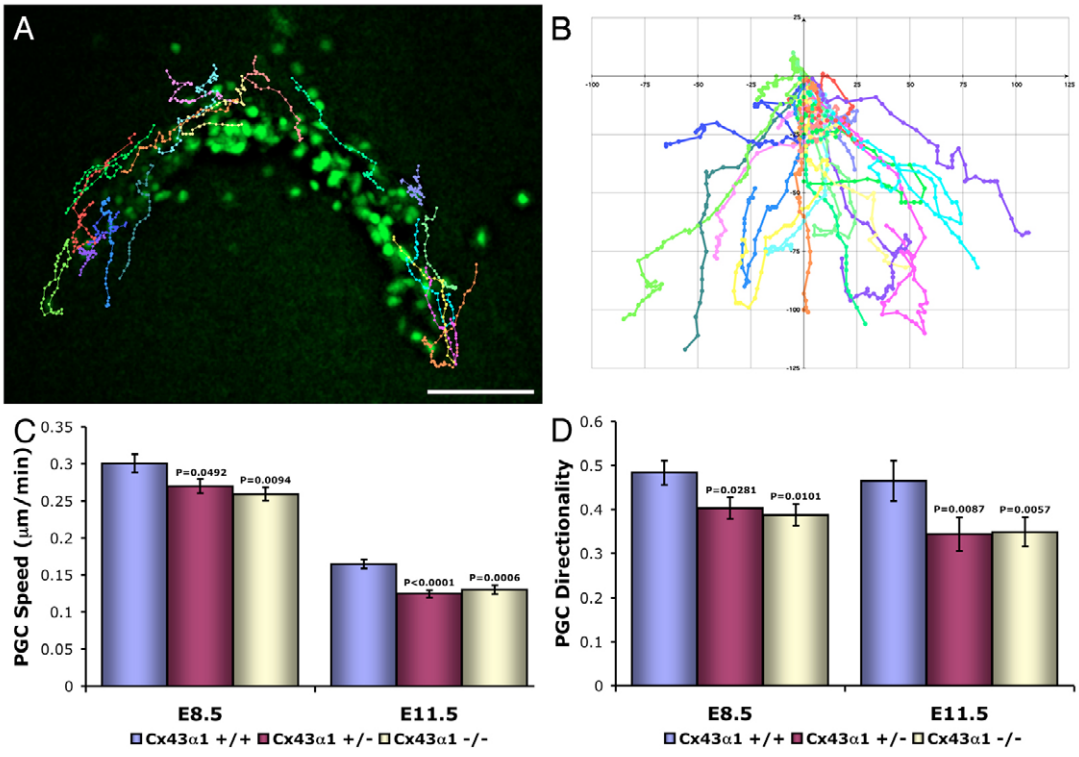

Fig. 3. Analysis of PGC migration in Cx43α1KO mouse embryos. (**A**,**B**) An example of how GFP-expressing PGCs were visualized and tracked in an E8.5 mouse embryo by time-lapse imaging. The migratory paths of individual PGCs are superimposed on the image of the embryo seen at the beginning of the experiment (A), and for clarity are plotted with a single origin in B. (**C**,**D**) The migratory paths of PGCs in E8.5 and E11.5 embryos were used to determine the speed (C) and directionality (D) of cell locomotion. PGCs from both homozygous and heterozygous Cx43α1KO embryos demonstrated significant decreases in both speed and directionality. This data entailed the analysis of a total of 72 Cx43α1 +/+, 74 Cx43α1 +/– and 66 Cx43α1 –/– independent cell migration tracings obtained from five embryo explants for each of the three Cx43α1 genotypes. Scale bar: 100 μm.

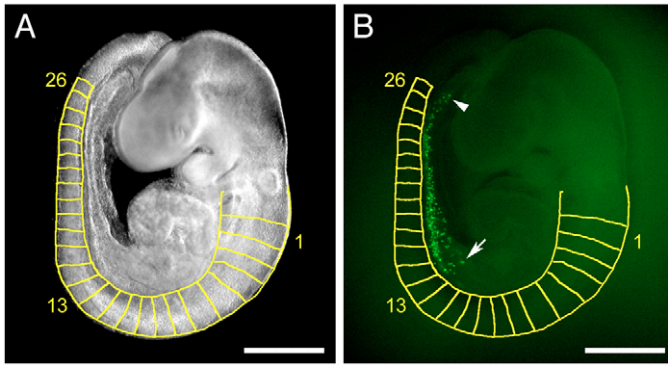

Fig. 4. PGC migration along the hindgut of Cx43α1KO embryos. Phase contrast (**A**) and GFP fluorescence (**B**) images of an E9.5 wild-type mouse embryo demonstrate the distribution of PGCs along the hindgut. We used somites as morphological landmarks (outlined in yellow) to assess the abundance of PGCs along the hindgut. We also determined the maximal PGC migration distance by measuring the distance from the base of the allantois (arrowhead), where PGCs originate, to the migration front situated rostrally along the anterior hindgut (arrow). Scale bars: 1 mm.

contrast to the increase in apoptosis of PGCs, no difference was found for PGC cell proliferation (Fig. 6A-C). Overall, these results suggest that increased apoptosis probably plays a significant role in PGC deficiency in the Cx43α1 KO mouse embryos.

β1 integrin in PGC migration

As integrin-mediated adhesion is known to play an important role in cell migration and cell survival, we further examined the role of β1 integrin in PGC migration. β1 integrin is expressed in migrating PGCs (De Felici et al., 2005) and can dimerize with a variety of α integrins to mediate cell adhesion to fibronectin and other extracellular matrices. Using time-lapse videomicroscopy, we examined the effects of a β1-integrin-function-blocking antibody on PGC migration in explants of E11.5 genital ridges. Treatment with a β1-integrin-function-blocking antibody significantly inhibited PGC migration, with reductions seen in both the speed and directionality of cell movement (Fig. 7A). To examine if β1-integrin function in PGCs may be affected by the loss of Cx43α1, we quantitatively assessed β1-integrin-mediated PGC adhesion. For these studies, PGCs isolated from the genital ridges of E11.5 embryos were plated in wells coated with a β1-integrin antibody. The efficiency of PGC attachment to the antibody-coated wells was quantitated to assess β1-integrin-mediated adhesion. These studies showed a significant reduction in adhesion of Cx43α1-deficient PGCs (Fig. 7B). By contrast, no differences were seen in control experiments with PGCs plated in wells coated with goat anti-mouse IgG antibody (Fig. 7B). Together these findings suggest that Cx43α1 expression is required for normal regulation of β1-integrin function.

Abnormal p53 activation and PGC apoptosis

Given that p53 is known to play a role in anoikis, a term for apoptosis elicited by the disruption of integrin-mediated adhesion, we examined the expression of activated p53 in PGCs using an antibody to phosphorylated Ser^{15}-p53 (Fig. 8A-C). Analysis showed a significant increase in activated p53 in PGCs of Cx43α1KO E11.5 genital ridges (Fig. 8C). To further evaluate the potential role of p53 activation in the increased apoptotic cell death of PGCs in the Cx43α1KO embryos, we examined the effects of α-pifithrin on PGC abundance and cell survival. Pifithrin is a p53 antagonist that can prevent apoptosis by blocking p53-dependent transcription (Komarov et al., 1999). Its effectiveness has been demonstrated in both in vitro and in vivo studies (Komarov et al., 1999; Pani et al., 2002). For our studies, pregnant dams were given two injections of pifithrin (2.2 mg/kg) 12 hours apart at approximately E10.5 and E11.0, with embryos harvested at E11.5. PGC abundance was subsequently assessed by monitoring GFP fluorescence in the genital ridges (Fig. 8D). In embryos obtained from the control vehicle injected dams, PGC abundance was indistinguishable from that previously observed in untreated E11.5 embryos. This included the expected reduction in PGC abundance in homozygous KO

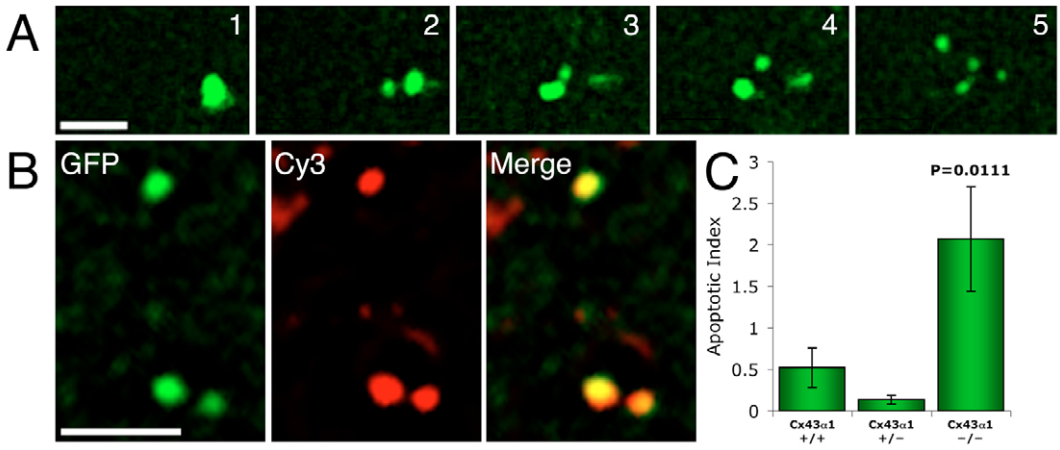

Fig. 5. PGC fragmentation seen by time-lapse imaging. (**A**) Images from a time-lapse series, showing the progressive fragmentation of a PGC seen in an E11.5 genital ridge explant from a homozygous Cx43α1KO mouse embryo. The images 1 through 5 are 24 minutes apart. (**B**) After time-lapse imaging, the genital ridges were stained with a sulforhodamine derivative of valylalanylaspartic acid fluoromethyl ketone that binds caspases 1, 3, 4, 5, 6, 7, 8 and 9 (see Cy3 panel). In the merged image, regions of co-localization of the polycaspase staining (Cy3 panel) with the PGC cell fragments (GFP panel) can be seen. (**C**) From analysis of the time-lapse movies, the number of apoptotic and mitotic cells was quantitated to generate an apoptotic index comprising the number of apoptotic cells normalized by the number of mitotic cells. This showed a significant increase in apoptosis in the homozygous Cx43α1KO genital ridges. The number of embryos used in this analysis included seven Cx43α1 +/+, four Cx43α1 +/– and five Cx43α1 –/– embryos. Scale bars: 25 μm.

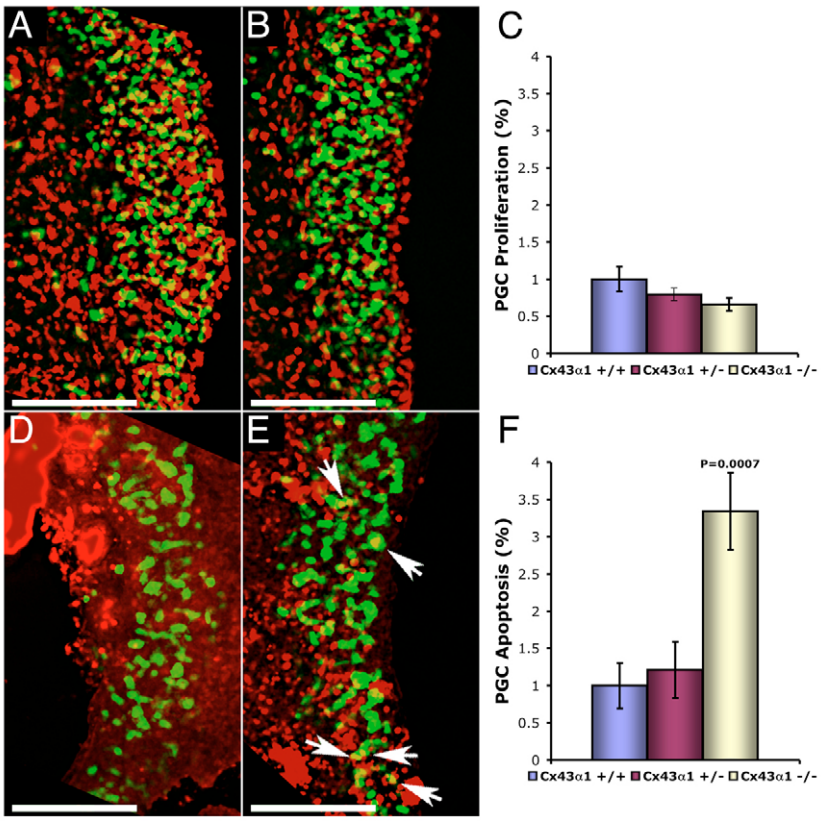

Fig. 6. PGC apoptosis and proliferation in E11.5 genital ridges. (**A-C**) BrdU labeling was used to assess the cell proliferation rate of PGCs in E11.5 wild-type (A) heterozygous and homozygous Cx43α1KO (B) embryos. BrdU immunodetection using an Alexa Fluor 546 conjugated anti-BrdU antibody (red) showed some regions of co-localization with GFP-expressing PGCs (seen as yellow). No statistical difference was seen in the proliferation rate of PGCs in wild-type versus heterozygous/homozygous Cx43α1KO mouse embryos (C). Note that the data are normalized to the frequency of BrdU-positive PGCs in wild-type embryos. This analysis included eight Cx43α1 +/+, 25 Cx43α1 +/– and six Cx43α1 –/– genital ridges. (**D-F**) TUNEL labeling in E11.5 genital ridges from wild-type (D) and Cx43α1KO (E) mouse embryos. TUNEL labeling is visualized by BrdU incorporation, detected using Alexa Fluor 546 conjugated anti-BrdU antibody (red). In the genital ridges from the KO mouse embryo, we noted many regions containing TUNEL-positive GFP-expressing PGCs (see white arrows in E). Quantitative assessments showed a significant increase in TUNEL-positive PGCs in the homozygous Cx43α1KO embryos (F). Note that the data are normalized to the frequency of TUNEL-positive PGCs in wild-type embryos. This analysis included 12 Cx43α1 +/+, 16 Cx43α1 +/– and 10 Cx43α1 –/– genital ridges. Scale bars: 100 μm.

embryos (Table 1, Fig. 8D). By contrast, in the pifithrin-injected mice, there was an apparent rescue of PGCs in the homozygous Cx43α1KO mice. Thus PGC abundance was not significantly different between Cx43α1 wild-type, heterozygous or homozygous KO mouse embryos derived from pifithrin-injected dams (Fig. 8D). Further analysis by TUNEL labeling showed that apoptosis of Cx43α1KO PGCs was suppressed, as the incidence of PGC apoptosis in homozygous KO embryos was similar to that seen in wild-type and heterozygous KO embryos (Fig. 8E). In addition, analysis using an anti-phosphohistone H3 antibody showed no significant difference in the rate of PGC proliferation in pifithrin-treated embryos regardless of Cx43α1 genotype (data not shown). These findings suggest that PGC apoptosis in Cx43α1KO mouse embryos involves the abnormal elevation of p53 activation.

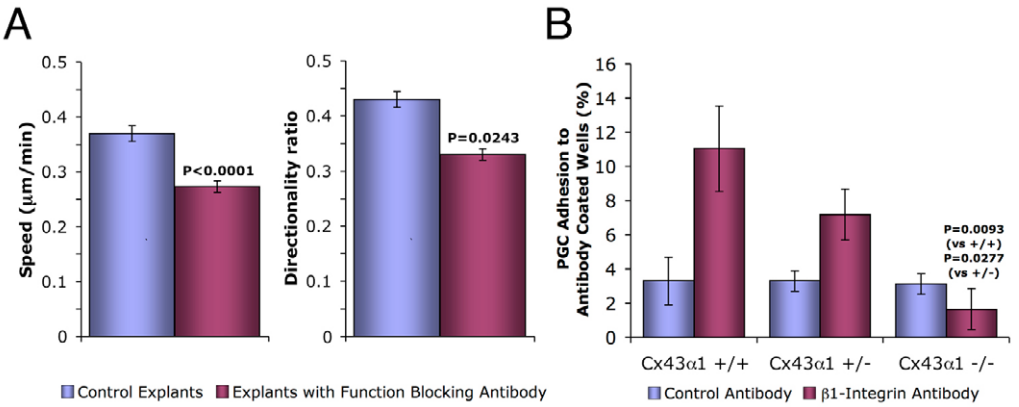

Fig. 7. Analysis of β1-integrin function in PGC motility. (**A**) Treatment of wild-type PGCs with a β1-integrin-function-blocking antibody caused a significant reduction in both the speed and directionality of PGC migration in E11.5 genital ridge explants. The migration data was obtained from the analysis of 48 cells derived from five embryo explants for both sham and function-blocking antibody treatments. (**B**) PGC attachment to β1-integrin-antibody-coated dishes was used to assess β1-integrin-mediated cell adhesion. Homozygous Cx43α1KO PGCs showed a marked reduction in β1-integrin-mediated adhesion, while control assays using plates coated with anti-mouse IgG antibodies showed no difference in adhesion between the different genotypes. It should be noted that the heterozygous KO PGCs also showed some reduction in adhesion to β1-integrin-antibody-coated dishes, but less than that observed in the homozygous KO PGCs. For assessments of β1-integrin-mediated adhesion, assays were carried out using PGCs derived from 14 Cx43α1 +/+, 20 Cx43α1 +/– and nine Cx43α1 –/– embryos, while control assays using anti-mouse IgG were carried out using PCGs from three Cx43α1 +/+, 14 Cx43α1 +/– and eight Cx43α1 –/– embryos.

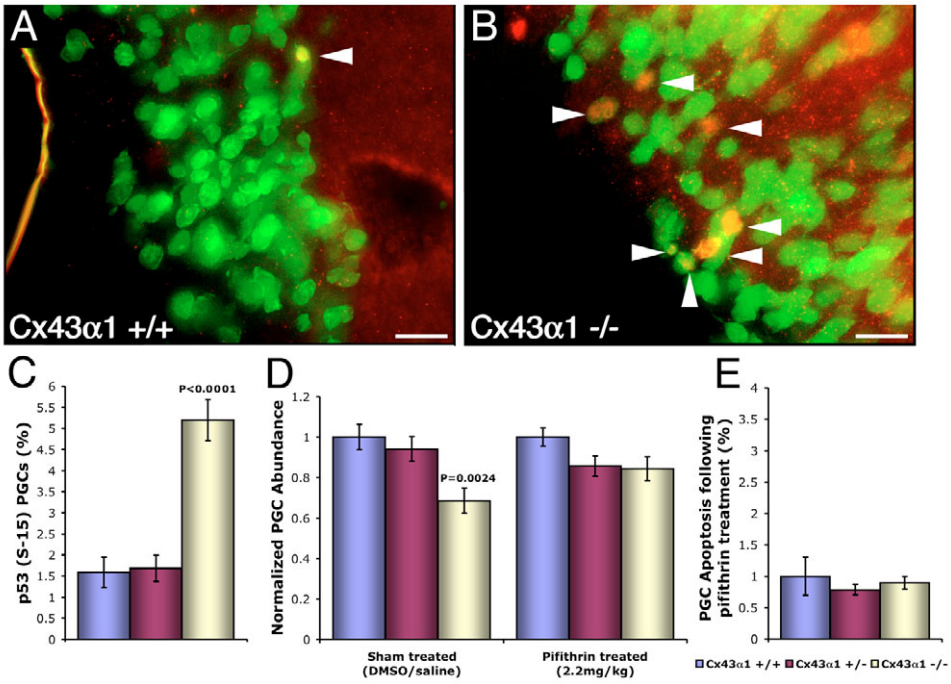

Fig. 8. Abnormal p53 activation in Cx43α1KO PGCs. (**A-C**) Genital ridges from E11.5 wild-type and Cx43α1KO mouse embryos were whole-mount stained using antibody against activated p53 (phospho-serine 15). PGCs (green) expressing activated p53 (red) are denoted by arrowheads. Quantitative analysis (C) revealed a marked increase in the expression of activated p53 in homozygous Cx43α1KO PGCs. This analysis was carried out using nine Cx43α1 +/+, 16 Cx43α1 +/– and 11 Cx43α1 –/– explants. (**D**) Assessment of PGC abundance in E11.5 genital ridges obtained from embryos of mice injected with α-pifithrin or with vehicle alone (DMSO). With vehicle injection, homozygous Cx43α1KO mouse embryos showed a significant reduction in PGC abundance. By contrast, following α-pifithrin treatment there was no difference in PGC abundance in the wild-type versus heterozygous or homozygous KO embryos. This analysis included 22 Cx43α1 +/+, 28 Cx43α1 +/– and ten Cx43α1 –/– α-pifithrin-treated embryos, and 15 Cx43α1 +/+, 18 Cx43α1 +/– and ten Cx43α1 –/– vehicle-treated embryos. (**E**) TUNEL labeling showed that following α-pifithrin treatment the rate of apoptosis was similar in homozygous KO, heterozygous KO or wild-type PGCs. Note that the data are normalized to the frequency of TUNEL-positive PGCs detected in wild-type embryos. This analysis included five Cx43α1 +/+, 37 Cx43α1 +/– and 16 Cx43α1 –/– α-pifithrin-treated genital ridges. Scale bars: 25 μm.

DISCUSSION

Our studies revealed no difference in PGC abundance between wild-type, heterozygous and homozygous Cx43α1KO embryos between E8.5 and E10.5. Thus specification of the germ cell lineage is probably unaffected by the loss of Cx43α1. However, PGC abundance at E11.5 was markedly reduced in the homozygous KO embryos. Although a reduction in the speed and directionality of cell movement was observed in the Cx43α1-deficient PGCs, heterozygous and homozygous KO PGCs showed similar changes in cell motility. This would argue against cell motility defects as a major contributing factor in the PGC deficiency, which is seen only in homozygous KO embryos. Consistent with this, we found no change in the overall distribution or in the maximal migration distance of PGCs in the hindgut of E9.5 Cx43α1KO embryos. This discrepancy may reflect the three or more days for PGC migration to the genital ridge, a very wide window of time that may mask the small difference in cell motile behavior exhibited by the heterozygous and homozygous Cx43α1KO PGCs. Together these findings suggest that the targeting of PGC to the genital ridge is not significantly affected by Cx43α1 deficiency.

Instead, our studies indicated an increase in apoptosis as the major factor causing germ cell loss in the E11.5 Cx43α1-deficient embryo. This was evident from the analysis of time-lapse movies, which showed fragmenting PGCs that later were found to be caspase positive. We also found increased apoptosis by direct TUNEL labeling of PGCs in homozygous Cx43α1KO embryos. By contrast, analysis of BrdU incorporation showed no change in the rate of PGC proliferation. Together these findings show that Cx43α1 is required for PGC survival in the genital ridge at E11.5. It is possible that the persistence of even a modest increase in the level of PGC apoptosis over time could account for the severe PGC deficiency seen at birth (Juneja et al., 1999), a possibility that will need to be further investigated in future studies.

We note that a number of mouse mutations have been identified that affect germ cell survival, the best characterized being those involving mutations in c-kit and the c-kit ligand, stem cell factor (SCF) (Bendel-Stenzel et al., 1998). These mutants exhibit a triad of anomalies that include spotting phenotype related to melanocyte defect, germ cell deficiency and hematopoietic defects. Although Cx43α1KO mice are not known to have pigmentation defects, we have observed ectopic pigment cells in the heart of Cx43α1KO mice (C.W.L., unpublished). In addition, recent studies suggest that Cx43α1 also may be important in hematopoiesis, perhaps through mediating stromal-dependent interactions (Cancelas et al., 2000; Durig et al., 2000; Ploemacher et al., 2000). Together with the germ cell deficiency, this would suggest the intriguing possibility that Cx43α1 regulation of PGC survival may entail downstream signaling involving c-kit. Given that PGCs are gap junction communication competent, this could be mediated via direct transfer of second messengers, metabolites, and even peptides between cells

(Bruzzone et al., 1996; Neijssen et al., 2005), and could involve direct coupling of PGCs with PGCs, or PGCs with somatic cells. Although our dye-coupling analysis did not detect dye transfer between PGCs, PGCs are extensively networked via direct cell-cell contacts, and gap junctional communication between PGCs cannot be ruled out (Gomperts et al., 1994).

Given the important role of integrins in modulating cell motility and cell survival, we also examined integrin function in migrating PGCs. We note that a number of previous studies have suggested that gap junctions and integrins may be coordinately regulated. For example, β1-integrin loss following RGD peptide treatment was associated with dysregulated expression of Cx43α1 (Czyz et al., 2005). Another study showed that Cx43α1 gap junctions were lost when cells were treated with antibodies against fibronectin or integrin (Guo et al., 2002). Using β1-integrin-function-blocking antibody, we showed that β1-integrin is required for PGC motility. In Cx43α1-deficient PGCs, we found a reduction in β1-integrin-mediated adhesion. These observations suggested the possibility that the loss of PGCs may involve anoikis – cell death elicited by perturbation of integrin-mediated adhesion. Cx43α1-deficient PGCs were also found to have elevated expression of activated p53, which is known to play an important role in anoikis (Grossmann, 2002). Moreover, pifithrin, a p53 antagonist, prevented the apoptotic loss of PGCs in the Cx43α1KO embryos. Together these findings suggest that Cx43α1 regulation of PGC cell survival involves downstream regulation of p53 cell signaling. Recent studies suggest that p53 translocation into the mitochondria may be an important initial step in p53-mediated induction of apoptosis (Zhao et al., 2005). Interestingly, Cx43α1 also has been shown to translocate into the mitochondria (Schulz and Heusch, 2004), and this has been suggested to protect against ischemic cell death (Boengler et al., 2005). Whether Cx43α1 and p53 are translocated into the mitochondria in PGCs undergoing apoptosis is not known.

The unique property of gap junctions in providing a conduit for the direct coupling of metabolic pools between cells makes a compelling argument for gap-junction-mediated cell-cell communication playing a role in apoptosis. Treatment of well-coupled GFSHR-17 granulosa cells with gap junction uncouplers has been reported to promote apoptosis (Ngezahayo et al., 2005). However, in primary granulosa cells, the induction of apoptosis was actually associated with increased cell coupling, and upon gap junction blockade, apoptosis was inhibited (Krysko et al., 2004). We note that a specific role for Cx43α1 in apoptosis has been suggested in a number of other studies (Albright et al., 2001; Furlan et al., 2001; Nakase et al., 2004; Yasui et al., 2000). Thus Cx43α1 knockdown using antisense was shown to elicit apoptosis in cultured rat cardiomyocytes (Yasui et al., 2000), while another study showed cell surface expression of Cx43α1 inhibited apoptosis induced by choline deficiency (Albright et al., 2001). Elevated apoptosis was also found in conjunction with focal ischemic brain injury in mice with astrocyte-targeted deletion of Cx43α1 (Nakase et al., 2004). In contrast to these findings, several studies showed that ectopic Cx43α1 expression is positively correlated with apoptosis (Huang et al., 2001; Hur et al., 2003; Kalvelyte et al., 2003). Thus the precise role of gap-junction-mediated coupling in modulating apoptosis remains unclear, and potentially could be cell and tissue context-dependent.

Overall, our studies indicate that apoptosis underlies the germ cell deficiency of the Cx43α1KO mouse. Our findings suggest that this may involve anoikis and the abnormal activation of p53 elicited by altered integrin function in the Cx43α1-deficient PGCs. How integrin function may be modulated by Cx43α1 and whether this involves signaling mediated by gap-junctional coupling and/or Cx43α1-mediated protein-protein interactions are challenging questions that will need to be addressed in future studies. It is interesting to note that recent reports have suggested that gap-junctional coupling may not be essential to the modulation of cell motility and cell proliferation by Cx43α1 (Huang et al., 1998; Moorby and Patel, 2001; Qin et al., 2002; Xu et al., 2001). Whether these findings have any relevance to apoptosis will need to be investigated in future studies.

We thank Dr H. R. Scholer for providing the *Oct4-GFP* transgenic mouse line. This work was supported by funding from the Division of Intramural Research of National Heart Lung Blood Institute/National Institutes of Health.

Supplementary material

Supplementary material for this article is available at
http://dev.biologists.org/cgi/content/full/133/17/3451/DC1

References

Albright, C. D., Kuo, J. and Jeong, S. (2001). cAMP enhances Cx43 gap junction formation and function and reverses choline deficiency apoptosis. *Exp. Mol. Pathol.* **71**, 34-39.

Bendel-Stenzel, M., Anderson, R., Heasman, J. and Wylie, C. (1998). The origin and migration of primordial germ cells in the mouse.[comment]. *Semin. Cell Dev. Biol.* **9**, 393-400.

Boengler, K., Dodoni, G., Rodriguez-Sinovas, A., Cabestrero, A., Ruiz-Meana, M., Gres, P., Konietzka, I., Lopez-Iglesias, C., Garcia-Dorado, D., Di Lisa, F. et al. (2005). Connexin 43 in cardiomyocyte mitochondria and its increase by ischemic preconditioning. *Cardiovasc. Res.* **67**, 234-244.

Bruzzone, R., White, T. W. and Paul, D. L. (1996). Connections with connexins: the molecular basis of direct intercellular signaling. *Eur. J. Biochem.* **238**, 1-27.

Cancelas, J. A., Koevoet, W. L., de Koning, A. E., Mayen, A. E., Rombouts, E. J. and Ploemacher, R. E. (2000). Connexin-43 gap junctions are involved in multiconnexin-expressing stromal support of hemopoietic progenitors and stem cells. *Blood* **96**, 498-505.

Czyz, J., Guan, K., Zeng, Q. and Wobus, A. M. (2005). Loss of beta1 integrin function results in upregulation of connexin expression in embryonic stem cell-derived cardiomyocytes. *Int. J. Dev. Biol.* **49**, 33-41.

De Felici, M., Scaldaferri, M. L. and Farini, D. (2005). Adhesion molecules for mouse primordial germ cells. *Front. Biosci.* **10**, 542-551.

Durig, J., Rosenthal, C., Halfmeyer, K., Wiemann, M., Novotny, J., Bingmann, D., Duhrsen, U. and Schirrmacher, K. (2000). Intercellular communication between bone marrow stromal cells and CD34+ haematopoietic progenitor cells is mediated by connexin 43-type gap junctions. *Br. J. Haematol.* **111**, 416-425.

Furlan, F., Lecanda, F., Screen, J. and Civitelli, R. (2001). Proliferation, differentiation and apoptosis in connexin43-null osteoblasts. *Cell Commun. Adhes.* **8**, 367-371.

Ginsburg, M., Snow, M. H. and McLaren, A. (1990). Primordial germ cells in the mouse embryo during gastrulation. *Development* **110**, 521-528.

Gittens, J. E. and Kidder, G. M. (2005). Differential contributions of connexin37 and connexin43 to oogenesis revealed in chimeric reaggregated mouse ovaries. *J. Cell Sci.* **118**, 5071-5078.

Gittens, J. E., Mhawi, A. A., Lidington, D., Ouellette, Y. and Kidder, G. M. (2003). Functional analysis of gap junctions in ovarian granulosa cells: distinct role for connexin43 in early stages of folliculogenesis. *Am. J. Physiol. Cell Physiol.* **284**, C880-C887.

Gomperts, M., Garcia-Castro, M., Wylie, C. and Heasman, J. (1994). Interactions between primordial germ cells play a role in their migration in mouse embryos. *Development* **120**, 135-141.

Goodenough, D. A., Goliger, J. A. and Paul, D. L. (1996). Connexins, connexons, and intercellular communication. *Annu. Rev. Biochem.* **65**, 475-502.

Grossmann, J. (2002). Molecular mechanisms of 'detachment-induced apoptosis–Anoikis'. *Apoptosis* **7**, 247-260.

Guo, Y., Martinez-Williams, C. and Rannels, D. E. (2002). Integrin-mediated regulation of connexin 43 expression by alveolar epithelial cells. *Chest* **121**, 30S-31S.

Huang, G. Y., Cooper, E. S., Waldo, K., Kirby, M. L., Gilula, N. B. and Lo, C. W. (1998). Gap junction-mediated cell-cell communication modulates mouse neural crest migration. *J. Cell Biol.* **143**, 1725-1734.

Huang, R. P., Hossain, M. Z., Huang, R., Gano, J., Fan, Y. and Boynton, A. L. (2001). Connexin 43 (cx43) enhances chemotherapy-induced apoptosis in human glioblastoma cells. *Int. J. Cancer* **92**, 130-138.

Hur, K. C., Shim, J. E. and Johnson, R. G. (2003). A potential role for cx43-hemichannels in staurosporin-induced apoptosis. *Cell Commun. Adhes.* **10**, 271-277.

Juneja, S. C., Barr, K. J., Enders, G. C. and Kidder, G. M. (1999). Defects in the germ line and gonads of mice lacking connexin43. *Biol. Reprod.* **60**, 1263-1270.
Kalvelyte, A., Imbrasaite, A., Bukauskiene, A., Verselis, V. K. and Bukauskas, F. F. (2003). Connexins and apoptotic transformation. *Biochem. Pharmacol.* **66**, 1661-1672.
Kawase, E., Hashimoto, K. and Pedersen, R. A. (2004). Autocrine and paracrine mechanisms regulating primordial germ cell proliferation. *Mol. Reprod. Dev.* **68**, 5-16.
Komarov, P. G., Komarova, E. A., Kondratov, R. V., Christov-Tselkov, K., Coon, J. S., Chernov, M. V. and Gudkov, A. V. (1999). A chemical inhibitor of p53 that protects mice from the side effects of cancer therapy. *Science* **285**, 1733-1737.
Krysko, D. V., Mussche, S., Leybaert, L. and D'Herde, K. (2004). Gap junctional communication and connexin43 expression in relation to apoptotic cell death and survival of granulosa cells. *J. Histochem. Cytochem.* **52**, 1199-1207.
Kumar, N. M. and Gilula, N. B. (1996). The gap junction communication channel. *Cell* **84**, 381-388.
Li, W. E., Waldo, K., Linask, K. L., Chen, T., Wessels, A., Parmacek, M. S., Kirby, M. L. and Lo, C. W. (2002). An essential role for connexin43 gap junctions in mouse coronary artery development. *Development* **129**, 2031-2042.
McLaren, A. (2003). Primordial germ cells in the mouse. *Dev. Biol.* **262**, 1-15.
Molyneaux, K. A., Stallock, J., Schaible, K. and Wylie, C. (2001). Time-lapse analysis of living mouse germ cell migration. *Dev. Biol.* **240**, 488-498.
Moorby, C. and Patel, M. (2001). Dual functions for connexins: Cx43 regulates growth independently of gap junction formation. *Exp. Cell Res.* **271**, 238-248.
Nakase, T., Sohl, G., Theis, M., Willecke, K. and Naus, C. C. (2004). Increased apoptosis and inflammation after focal brain ischemia in mice lacking connexin43 in astrocytes. *Am. J. Pathol.* **164**, 2067-2075.
Neijssen, J., Herberts, C., Drijfhout, J. W., Reits, E., Janssen, L. and Neefjes, J. (2005). Cross-presentation by intercellular peptide transfer through gap junctions. *Nature* **434**, 83-88.
Ngezahayo, A., Altmann, B., Steffens, M. and Kolb, H. A. (2005). Gap junction coupling and apoptosis in GFSHR-17 granulosa cells. *J. Membr. Biol.* **204**, 137-144.
Pani, L., Horal, M. and Loeken, M. R. (2002). Rescue of neural tube defects in Pax-3-deficient embryos by p53 loss of function: implications for Pax-3-dependent development and tumorigenesis. *Genes Dev.* **16**, 676-680.
Perez-Armendariz, E. M., Lamoyi, E., Mason, J. I., Cisneros-Armas, D., Luu-The, V. and Bravo Moreno, J. F. (2001). Developmental regulation of connexin 43 expression in fetal mouse testicular cells. *Anat. Rec.* **264**, 237-246.
Perez-Armendariz, E. M., Saez, J. C., Bravo-Moreno, J. F., Lopez-Olmos, V., Enders, G. C. and Villalpando, I. (2003). Connexin43 is expressed in mouse fetal ovary. *Anat. Rec. A Discov. Mol. Cell. Evol. Biol.* **271**, 360-367.
Pesce, M. and Scholer, H. R. (2001). Oct-4: gatekeeper in the beginnings of mammalian development. *Stem Cells* **19**, 271-278.
Ploemacher, R. E., Mayen, A. E., De Koning, A. E., Krenacs, T. and Rosendaal, M. (2000). Hematopoiesis: gap junction intercellular communication is likely to be involved in regulation of stroma-dependent proliferation of hemopoietic stem cells. *Hematology* **5**, 133-147.
Qin, H., Shao, Q., Curtis, H., Galipeau, J., Belliveau, D. J., Wang, T., Alaoui-Jamali, M. A. and Laird, D. W. (2002). Retroviral delivery of connexin genes to human breast tumor cells inhibits in vivo tumor growth by a mechanism that is independent of significant gap junctional intercellular communication. *J. Biol. Chem.* **277**, 29132-29138.
Reaume, A. G., de Sousa, P. A., Kulkarni, S., Langille, B. L., Zhu, D., Davies, T. C., Juneja, S. C., Kidder, G. M. and Rossant, J. (1995). Cardiac malformation in neonatal mice lacking connexin43.[comment]. *Science* **267**, 1831-1834.
Roscoe, W. A., Barr, K. J., Mhawi, A. A., Pomerantz, D. K. and Kidder, G. M. (2001). Failure of spermatogenesis in mice lacking connexin43. *Biol. Reprod.* **65**, 829-838.
Schulz, R. and Heusch, G. (2004). Connexin 43 and ischemic preconditioning. *Cardiovasc. Res.* **62**, 335-344.
Sohl, G. and Willecke, K. (2004). Gap junctions and the connexin protein family. *Cardiovasc. Res.* **62**, 228-232.
Sullivan, R., Huang, G. Y., Meyer, R. A., Wessels, A., Linask, K. K. and Lo, C. W. (1998). Heart malformations in transgenic mice exhibiting dominant negative inhibition of gap junctional communication in neural crest cells. *Dev. Biol.* **204**, 224-234.
Tam, P. P. and Snow, M. H. (1981). Proliferation and migration of primordial germ cells during compensatory growth in mouse embryos. *J. Embryol. Exp. Morphol.* **64**, 133-147.
Wang, W. J., Kuo, J. C., Yao, C. C. and Chen, R. H. (2002). DAP-kinase induces apoptosis by suppressing integrin activity and disrupting matrix survival signals. *J. Cell Biol.* **159**, 169-179.
White, T. W. and Paul, D. L. (1999). Genetic diseases and gene knockouts reveal diverse connexin functions. *Annu. Rev. Physiol.* **61**, 283-310.
Xu, X., Li, W. E., Huang, G. Y., Meyer, R., Chen, T., Luo, Y., Thomas, M. P., Radice, G. L. and Lo, C. W. (2001). Modulation of mouse neural crest cell motility by N-cadherin and connexin 43 gap junctions. *J. Cell Biol.* **154**, 217-230.
Yasui, K., Kada, K., Hojo, M., Lee, J. K., Kamiya, K., Toyama, J., Opthof, T. and Kodama, I. (2000). Cell-to-cell interaction prevents cell death in cultured neonatal rat ventricular myocytes. *Cardiovasc. Res.* **48**, 68-76.
Yoshimizu, T., Sugiyama, N., De Felice, M., Yeom, Y. I., Ohbo, K., Masuko, K., Obinata, M., Abe, K., Scholer, H. R. and Matsui, Y. (1999). Germline-specific expression of the Oct-4/green fluorescent protein (GFP) transgene in mice. *Dev. Growth Differ.* **41**, 675-684.
Yoshimizu, T., Obinata, M. and Matsui, Y. (2001). Stage-specific tissue and cell interactions play key roles in mouse germ cell specification. *Development* **128**, 481-490.
Zhang, Y., Lu, H., Dazin, P. and Kapila, Y. (2004). Squamous cell carcinoma cell aggregates escape suspension-induced, p53-mediated anoikis: fibronectin and integrin alphav mediate survival signals through focal adhesion kinase. *J. Biol. Chem.* **279**, 48342-48349.
Zhao, Y., Chaiswing, L., Velez, J. M., Batinic-Haberle, I., Colburn, N. H., Oberley, T. D. and St Clair, D. K. (2005). p53 translocation to mitochondria precedes its nuclear translocation and targets mitochondrial oxidative defense protein-manganese superoxide dismutase. *Cancer Res.* **65**, 3745-3750.